2012

The Replication of a Lotus Leaf Surface Using Neat, Rubber-Modified and Nanosilica Modified Epoxies

Maria Salamon
Lehigh University

THE REPLICATION OF A LOTUS LEAF SURFACE USING NEAT, RUBBER-MODIFIED AND NANOSILICA MODIFIED EPOXIES

by

Maria Martine Salamon

A Thesis

Presented to the Graduate and Research Committee

of Lehigh University

in Candidacy for the Degree of

Master of Science

in

Polymer Science and Engineering

Lehigh University

September, 2012

CERTIFICATE OF APPROVAL

This thesis is accepted and approved in partial fulfillment of the requirements for the Master of Science.

_____
Date

_____
Thesis Advisor
Director, PSE Graduate Program

DEDICATION

To my grandparents.

ACKNOWLEDGEMENTS

Success in graduate school is not achieved without the help of many, many persons. In an effort to keep this short and sweet, I will limit my formal acknowledgements to those who had a direct impact on this work alone.

I would like to thank my advisor Dr. Raymond A. Pearson, for giving me a place in the Polymer Science and Engineering Department. For this I will be forever grateful, both for the opportunity to study at Lehigh University as a graduate student and for all of the knowledge and experience I gained since being a group member.

I wish to thank my boss at Research Support Instruments, John F. Kline, for giving life to this project and encouraging me to pursue it. I am also deeply grateful for both his patience with my schedule and support of all of my research activities. Thank you to my co-worker at Research Support Instruments, Dr. Daniel J. Sullivan, for his ebullient encouragement and for introducing me to image analysis and numerous software programs that were so essential to the completion of this work.

Thank you, Lauren Bacigalupo, for teaching me everything I know about how to process epoxies. This project would not exist without your training. Thank you to Bill Mushock for all of his help with the scanning electron microscopy work.

I want to thank my parents, John and Mary Salamon, for their strenuous support, my friends Deb and Sophia for their continual prayers and Patty for letting me gripe about the travails of research.

Finally, I thank God, with Whom all things are possible.

TABLE OF CONTENTS

TITLE PAGE……..i

CERTIFICATE OF APPROVAL……ii

DEDICATION…….……..……...……iii

ACKNOWLEDGEMENTS…….....……iv

TABLE OF CONTENTS……v

LIST OF TABLES…….…….vii

LIST OF FIGIURES……...……...viii

ABSTRACT……....1

CHAPTER

1. **INTRODUCTION**……...……...……..2

1.1 Surface Structure and Composition of the *Nelumbo nucifera* Leaf…..2

1.2 The Lotus Effect…….……..3

1.3 Wetting…….5

1.4 Biomimetic Lotus-like Surfaces…...……7

1.5 Replica Molding……7

2. **EXPERIMENTAL APPROACH**……....9

2.1 Preparation of Lotus Replica Mold……..9

2.2 Preparation of Epoxies……10

2.2.1 Neat Epoxy Resin……10

2.2.2 Rubber-Modified Epoxy Resin……..……..11

2.2.3 Nanosilica-Filled Epoxy Resin……..……....……12

2.3 Replica Molding of Epoxy Systems……...12

2.4 Formation of the Control Surface……...13

2.5 Contact Angle Measurement Procedure…….13

2.5.1 Image Analysis…….……14

2.6 Scanning Electron Microscopy……...14

2.7 Optical Profilometry……...15

3. **RESULTS**…….....16

3.1 Static Contact Angles……..16

3.2 Scanning Electron Microscopy Images of Lotus-Like Surfaces…….19

3.3 Profiles of Control Surfaces……24

4. **DISCUSSION**……..27

4.1 Replica Molding……..27

4.2 Optical Profilometry……...28

5. **SUMMARY**……30

6. **REFERENCES**……..31

7. **VITA**……34

LIST OF TABLES

Table 1.1 Summarizes the definitions of hydrophobicity and its relationship to the contact angle of water on a surface. All angles are expressed in degrees [15]..…….6

Table 2.1 Summarizes neat and rubber-modified epoxy formulations and their concentration…….10

Table 2.2 Summarizes all nanosilica modified epoxy formulations and their concentrations. The modifiers, epoxy resin and curing agent are described in more detail in sections 2.2.1-2.2.3……10

Table 3.1 Summarizes the average measured static contact angle and error for each epoxy formulation for both the flat (i.e. control) and lotus-molded surfaces……16

LIST OF FIGURES

Figure 1.1 A cross-sectional schematic illustrating the tertiary *Nelumbo nucifera* leaf structure. Convex cells on the epidermis have a length-to-width ratio such that they are considered papillose. Epicuticular waxes of different aquatic plants can assume different morphologies. In the case of *Nelumbo nucifera* nonacosanol waxes self-assemble into tubules……..3

Figure 1.2 A summary of static contact angles of water on the leaf surface of *Nelumbo nucifera* as reported in the literature. Values and error bars are as-provided from the corresponding journal article, which is cited in the graph legend [2, 10-15]…….**.....**4

Figure 1.3 A schematic illustrating how the energy of the liquid-air interface and ultimately the contact angle that a liquid forms with a surface results from the difference between the solid-air and solid-liquid interfacial surface energies [16]…….5

Figure 1.4 The graphic on the left illustrates the Wenzel model: homogeneous wetting of a drop on a surface. Note how the drop fills all features on the surface. The graphic on the right illustrates the Cassie-Baxter model: heterogeneous wetting of a drop on a surface. In this case the drop only wets the tallest surface features and air gaps are left between features and under the drop itself [17-18]…….6

Figure 3.1 Plot of the average static contact angle measurements for the neat and rubber modified epoxies, respectively. The error bars reflect the standard deviation. Please note that for points where the error bars are not readily apparent it means that the standard deviation was small enough to not be discernible on the scale presented…….17

Figure 3.2 Plot of the average static contact angle measurements for the neat and nanosilica modified epoxies, respectively. The error bars reflect the standard deviation. Please note that for points where the error bars are not readily apparent it means that the standard deviation was small enough to not be discernible on the scale presented……...18

Figure 3.3 Image of a neat epoxy/amine lotus leaf replica surface……..19

Figure 3.4 Close-up image of a neat epoxy/amine lotus replica papilla……..19

Figure 3.5 Image of a 5 phr CTBN/epoxy/amine lotus leaf replica surface……20

Figure 3.6 Close-up image of a 5 phr CTBN/epoxy/amine lotus replica papilla…….20

Figure 3.7 Image of a 10 phr CTBN/epoxy/amine lotus leaf replica surface……..21

Figure 3.8 Image of a 10 phr CTBN/epoxy/amine lotus leaf replica surface……..21

Figure 3.9 Image of a 0.66 wt% Nanosilica/epoxy/amine lotus leaf replica surface…...22

Figure 3.10 Image of a 1.3 wt% Nanosilica/epoxy/amine lotus leaf replica surface…...22

Figure 3.11 Image of a 2.56 wt% Nanosilica/epoxy/amine lotus leaf replica surface.....23

Figure 3.12 Image of a 4.93 wt% Nanosilica/epoxy/amine lotus leaf replica surface….23

Figure 3.13 Close-up image of a 4.93 wt% Nanosilica/epoxy/amine lotus replica papilla…….24

Figure 3.14 Optical profilometry results for a flat neat amine-cured epoxy system. The examined area is 2 mm x 2 mm. The step in the x-direction is 1 μm and the step in the y-direction is 100 μm. The profile plot is the average of 20 scans……..24

Figure 3.15 Optical profilometry results for a flat 0.66 wt% nanosilica-modified amine-cured epoxy system. The examined area is 2 mm x 2 mm. The step in the x-direction is 1 μm and the step in the y-direction is 5 μm. The profile plot is the average of 400 scans……...25

Figure 3.16 Optical profilometry results for a flat 1.3 wt% nanosilica-modified amine-cured epoxy system. The examined area is 2 mm x 2 mm. The step in the x-direction is 1 μm and the step in the y-direction is 5 μm. The profile plot is the average of 400 scans……...25

Figure 3.17 Optical profilometry results for a flat 4.93 wt% nanosilica-modified amine-cured epoxy system. The examined area is 2 mm x 2 mm. The step in the x-direction is 1 μm and the step in the y-direction is 100 μm. The profile plot is the average of 20 scans……..….25

Figure 3.18 Optical profilometry results for a flat 5 phr CTBN-modified amine-cured epoxy system. The examined area is 2 mm x 2 mm. The step in the x-direction is 1 μm and the step in the y-direction is 100 μm. The profile plot is the average of 20 scans…26

Figure 3.19 Optical profilometry results for a flat 10 phr CTBN-modified amine-cured epoxy system. The examined area is 2 mm x 2 mm. The step in the x-direction is 1 μm and the step in the y-direction is 100 μm. The profile plot is the average of 20 scans…26

Figure 3.20 Optical profilometry results for a flat 20 phr CTBN-modified amine-cured epoxy system. The examined area is 2 mm x 2 mm. The step in the x-direction is 1 μm and the step in the y-direction is 100 μm. The profile plot is the average of 20 scans….26

ABSTRACT

The lotus has long been the subject of investigation for its superhydrophobic leaves. Whereas most attempts to fabricate a lotus-like surface utilize human-designed structures, this work details the replication of the *Nelumbo nucifera* leaf surface with neat, CTBN-modified and nanosilica-modified epoxies via a molding process that uses the lotus leaf itself. It was found that this process was able to duplicate the micron-scale features of the lotus leaf. The replicated surface was thereafter examined using scanning electron microscopy and characterized for its surface wetting ability by static contact angle measurements. While none of the epoxy-based replicated lotus surfaces achieved the superhydrophobic contact angles evinced by actual *Nelumbo nucifera* leaves, such surfaces exhibited a significant increase in water contact angle of approximately 40 degrees over their flat counterparts.

CHAPTER 1

INTRODUCTION

It is reported in the literature that lotus leaves, specifically those of *Nelumbo nucifera*, remain superhydrophobic even with several days submersion under water [1]. The superhydrophobic lotus leaf surface, giving rise to the eponymously named "Lotus effect" is an archetypal example of surface chemistry and topography colluding to create a superhydrophobic surface. What follows is a demonstration of the alterability of the wetting properties of an epoxy surface, showing that it is not intrinsically limited to material surface chemistry but can be strongly influenced by surface topography. This is achieved through the formation of novel epoxy replicas of *Nelumbo nucifera* leaf surfaces.

1.1 Surface Structure and Composition of the *Nelumbo nucifera* Leaf

Nelumbo nucifera grows in an aquatic environment but its leaves rest on the surface of water. In order to allow plant respiration, inhibit mold spore germination and prevent infection, the plant must be able to control water accessibility to the leaf surface. The hierarchical structure of the upper surface of the *Nelumbo nucifera* leaf effectively discourages water retention and encourages particulate removal [2].

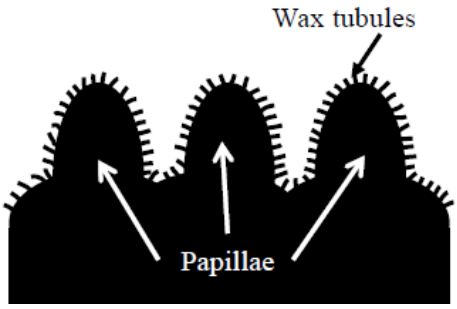

Figure 1.1 A cross-sectional schematic illustrating the tertiary *Nelumbo nucifera* leaf structure. Convex cells on the epidermis have a length-to-width ratio such that they are considered papillose. Epicuticular waxes of different aquatic plants can assume different morphologies. In the case of *Nelumbo nucifera* nonacosanol waxes self-assemble into tubules.

The tertiary structural hierarchy [3] of *Nelumbo nucifera* as illustrated in Figure 1.1 begins with convex epidermal cell morphology [4]. The epidermis is the outermost layer of plant tissue and it covers the entire plant except for the root structure. Epidermal cell width/height ratio is such that a secondary structure of papillose cells is evident [5]. These convex papillae have an average height of 13-15 μm [6] and a spatial density of approximately 3431 papillae/mm^2 [3]. The outermost surface of the epidermis is the cuticle, a biocomposite of cutin and waxes. In the case of *Nelumbo nucifera,* in addition to forming a thin epicuticular wax film over the cuticle [7], these nonacosanol waxes self-assemble into tubules [4, 8]. Tubules range in size from 0.3-1 μm in length, 80-120 nm in diameter and have a spatial density of 2.0 x 10^7 tubules/mm^2 [9].

1.2 The Lotus Effect

The term "Lotus effect" arose from the superhydrophic lotus leaf surface properties [2, 4-5, 9]. To wit, papillose leaf surface topography coupled with hydrophobic surface

chemistry presented by the nonacosanol wax tubules [4] results in heterogeneous wetting [9]. This gives rise to very large contact angles for water impinging on the surface with very little contact angle hysteresis [4-6, 9]. This is illustrated below in Figure 1.2.

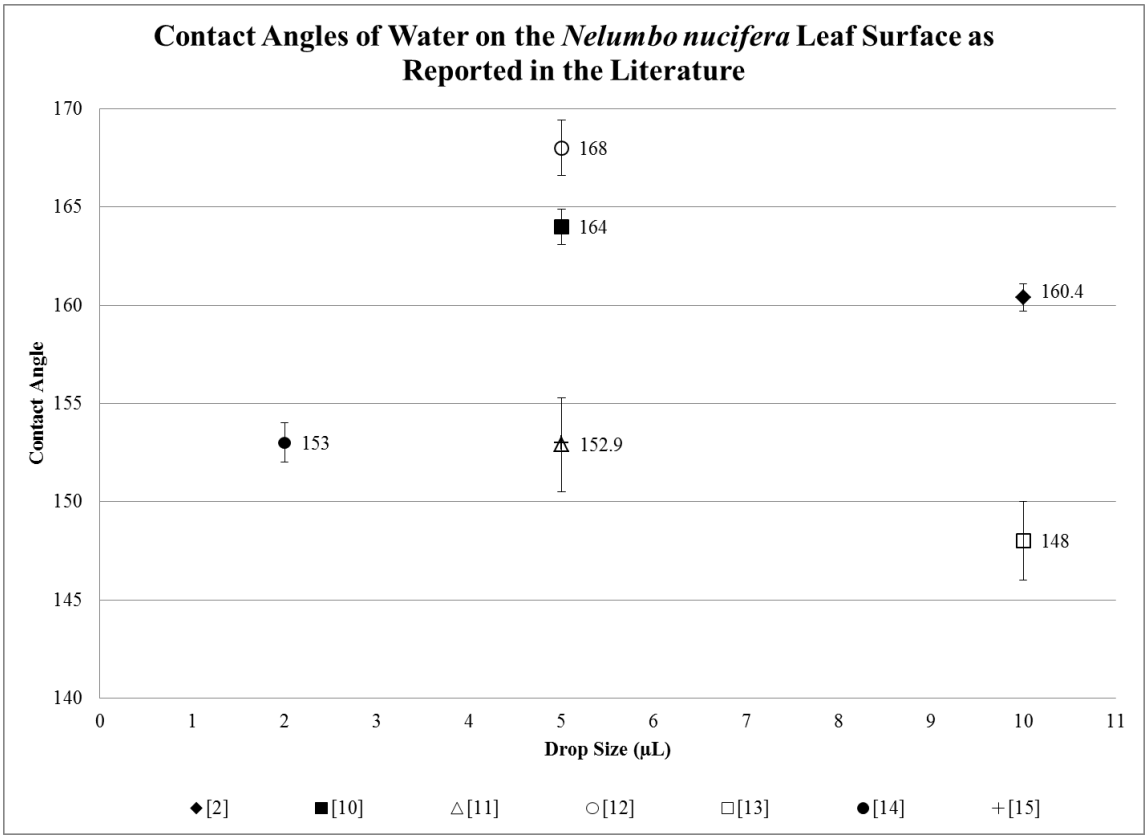

Figure 1.2 A summary of static contact angles of water on the leaf surface of *Nelumbo nucifera* as reported in the literature. Values and error bars are as-provided from the corresponding journal article, which is cited in the graph legend [2, 10-15].

Water impinging on the surface rolls off without wetting the surface and creates the "self-cleaning" effect by taking dust and dirt laying on the surface with it. In addition, water is inhibited from stagnating on the surface, thus discouraging pathogenic agents from residing on the plant [2].

1.3 Wetting

Wetting of liquids on a surface is intrinsically a function of the component surface energies. This is described by Young's Equation (Equation 1.1) where γ denotes the surface energies of solid-air, solid-liquid and liquid-air interfaces, respectively. The angle θ is measured at the point where a liquid drop edge contacts the surface. This is illustrated in Figure 1.3 below.

$$\gamma_{solid-air} - \gamma_{solid-liquid} = \gamma_{liquid-air} \cos\theta \tag{1.1}$$

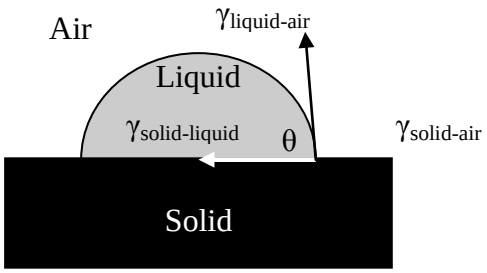

Figure 1.3 A schematic illustrating how the energy of the liquid-air interface and ultimately the contact angle that a liquid forms with a surface results from the difference between the solid-air and solid-liquid interfacial surface energies [16].

The surface energies themselves are a function of both surface chemistry and surface structure [15]. A higher surface energy material will give rise to a lower contact angle for a liquid on the surface than a lower surface energy material will [17]. This is respectively described phenomenologically as a hydrophilic or hydrophobic surface [15]; the contact angles for these terms are provided in the table below.

Table 1.1 Summarizes the definitions of hydrophobicity and its relationship to the contact angle of water on a surface. All angles are expressed in degrees [15].

Definition	Contact Angle
Hydrophilic	$\theta < 90$
Hydrophobic	$\theta > 90$ $\theta < 150$
Superhydrophobic	$\theta > 150$ $\theta \leq 180$

Surface structure also plays a crucial role in surface wetting. There are two basic wetting regimes: Wenzel, which describes homogeneous wetting of a surface, and Cassie-Baxter, which describes heterogeneous wetting of a surface [15, 17-18]. These are illustrated in Figure 1.4 below.

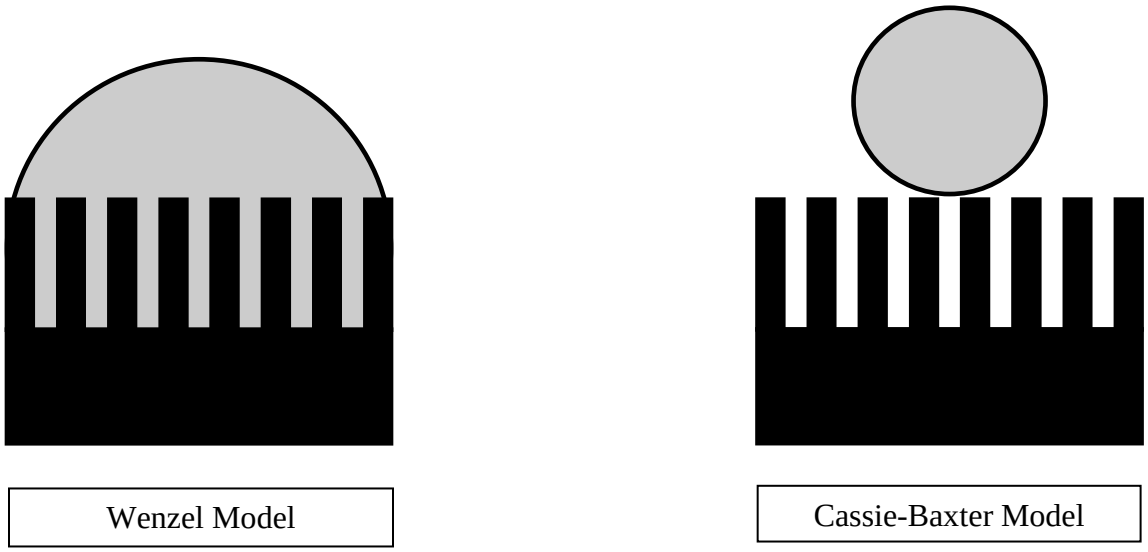

Figure 1.4 The graphic on the left illustrates the Wenzel model: homogeneous wetting of a drop on a surface. Note how the drop fills all features on the surface. The graphic on the right illustrates the Cassie-Baxter model: heterogeneous wetting of a drop on a surface. In this case the drop only wets the tallest surface features and air gaps are left between features and under the drop itself [17-18].

Homogeneous wetting implies that the liquid permeates all features on the surface. By contrast, heterogeneous wetting occurs when only the tips of surface features are wetted, and air gaps remain between the drop and the surface.

1.4 Biomimetic Lotus-like Surfaces

Given the excellent superhydrophobic surface properties of *Nelumbo nucifera* leaves, the morphology of the leaf often serves as a model for fabricated hydrophobic surfaces. Structures designed to mimic the lotus surface typically include: pillars of varying pitch and height [19], compound structures such that micron-scale features have a nano-featured surface [20-24], and chemical treatment in which case a hydrophobic material is deposited on a micro-patterned surface [25].

1.5 Replica molding

Replica molding is a technique widely used within the Microelectromechanical Systems (MEMS) research community. The basic premise is to cast a mold of the surface to be replicated using an elastomeric material-typically Poly(dimethylsiloxane) (PDMS). The viscosity of PDMS is low enough that when used as the mold material, micron-scale and nano-scale features are replicated with high fidelity [26]. One then fills the mold with the material of interest for duplicating the original and upon completion, a replica of the original is created.

Replica molding has been previously used to recreate the surface of a lotus leaf using the following as replicate materials: PDMS [27], lacquer [3], poly(methyl methacrylate) [11, 28-29], photopolymer RenShape SL 5180 [12], poly(ethylene oxide) [13], poly(caprolactone) [30], poly(vinyl chloride) [31], epoxy (Epoxydharz L®) [10] and polyether [32].

This work details the first use of rubber-modified and nanosilica-modified diglycidyl of bisphenol-A resins as the replica material.

CHAPTER 2

EXPERIMENTAL APPROACH

This chapter begins by delineating the replica molding process used in this study. Immediately thereafter, sample formulations are provided. The contact angle measurement procedures are detailed. The section concludes with a discussion of the image analysis methodology.

2.1 Preparation of a Lotus Replica Mold

Preparation of a lotus replica mold began with a fresh lotus leaf. In this study, the species used was *Nelumbo nucifera* (purchased from www.wildthingsgrow.com). A leaf was clipped from the plant, rinsed with tap water and gently patted dry with a lint-free clean room towel. The leaf was sectioned with a razor blade, discarding both the central stem and large veins of the plant. A leaf sample was secured using double-sided tape to an aluminum weigh tray such that the lower leaf surface was taped and the upper surface was open to the air.

Polydimethylsiloxane (PDMS) (Sylgard® 184) was thoroughly mixed in a 10:1 ratio of base resin to curing agent. Immediately thereafter, the mixture was placed in 32 mmHg vacuum until devoid of bubbles. The degassed mixture was poured over the lotus leaf and the filled weigh tray was placed in vacuum (maximum 100 mTorr) until bubbles stopped evolving from the mixture. At this time, the weigh tray was placed in a 40°C

oven for 4 hours. When the PDMS was no longer tacky and fully cured, the PDMS was peeled from the lotus leaf. Within the PDMS was a full negative of the lotus leaf surface.

2.2 Preparation of Epoxies

The epoxy systems under investigation in this study include neat, rubber modified and nanosilica-modified resins. While the additives and their concentrations differ the method of preparation was the same for each. Furthermore, the same batch of resin was used for both the lotus replica and control surfaces. Tables 2.1-2.2 below summarize all of the epoxy formulations.

Table 2.1 Summarizes neat and rubber-modified epoxy formulations and their concentration.

	Neat	**CTBN**	**CTBN**	**CTBN**
Modifer (grams)		0.75	1.5	3.0
Epoxy (grams)	15.0	15.0	15.0	15.0
Amine (grams)	6.0	6.0	6.0	6.0
Concentration (phr)	---	5	10	20

Table 2.2 Summarizes all nanosilica modified epoxy formulations and their concentrations. The modifiers, epoxy resin and curing agent are described in more detail in sections 2.2.1-2.2.3.

	Nanosilica	**Nanosilica**	**Nanosilica**	**Nanosilica**
Modifer (grams)	0.25	0.50	1.0	2.0
Epoxy (grams)	15.0	15.0	15.0	15.0
Amine (grams)	6.56	6.63	6.72	7.05
Concentration (weight percent)	0.66	1.3	2.56	4.93

2.2.1 Neat Epoxy Resin

A diglycidyl ether of bisphenol A (DGEBA) resin, DER 331 from Dow Chemical, was poured into a mixing jar. An aliphatic amine, Jeffamine T403 from Huntsman, was

added such that the ratio of epoxy to curing agent maintained a ratio of 40 parts curing agent to 100 parts epoxy. In this case the amount of epoxy used was 15 grams so 6 grams of amine was incorporated using constant hand-mixing for 3 minutes. The mixture was placed in 50 milliTorr vacuum until devoid of air bubbles; this process typically took no longer than 3 minutes.

2.2.2 Rubber-Modified Epoxy Resin

Rubber-modified resins were prepared in 3 different concentrations: 5 phr, 10 phr and 20 phr. The rubber modifier used was Hypro 1300X8 from Emerald Performance Materials, a carboxyl terminated butadiene-acrylonitrile (CTBN) reactive liquid random copolymer. For each concentration, 15 grams of epoxy was poured into a mixing jar. The 5 phr CTBN concentration required 0.75 grams of the rubber modifier, the 10 phr CTBN concentration required 1.5 grams of the rubber modifier and the 20 phr CTBN concentration required 3.0 grams of the rubber modifier. Each mixing jar was placed in an 80°C oven to encourage the dissolution of the rubber modifier into the epoxy, after which continuous hand-mixing was used for several minutes until the mixture was wholly uniform. The jars were allowed to cool to room temperature prior to adding 6 grams of amine to each jar. Continuous hand-mixing occurred for 3 minutes after which the jars were placed in 50 milliTorr vacuum until devoid of air bubbles.

2.2.3 Nanosilica-Filled Resin

Nanosilica-filled resins were prepared with the following additions of nanosilica (NS) to 15 grams each, respectively of epoxy: 0.25 grams, 0.50 grams, 1.0 grams and 2.0 grams. These additions resulted in concentrations of 0.66 wt%, 1.3 wt%, 2.56 wt% and 4.93 wt%. The concentration of nanosilica added was 40 weight % (Nanopox® F400). It was essential to heat the nanosilica-epoxy concentrate to not less than 80°C prior to adding it to the epoxy, in order to permit good incorporation of the nanosilica into the epoxy resin. Given that the nanosilica dispersion contains nanosilica previously dispersed in epoxy, it was necessary to account for the epoxy content of the nanosilica dispersion when calculating for the appropriate amount of amine curing agent. The amount of amine added to each concentration, respectively was 6.56 grams, 6.63 grams, 6.72 grams and 7.05 grams. Continuous hand-mixing occurred for 3 minutes after which the jars were placed in vacuum until devoid of air bubbles.

2.3 Replica Molding of Epoxy Systems

The PDMS negative of the lotus leaf was placed in an aluminum weigh tray such that the lotus negative was open to the air. Immediately after each epoxy formulation was fully degassed, it was removed from vacuum and poured over the PDMS mold, after which the filled molds were again placed in vacuum to a maximum of 190 milliTorr. The cessation of bubble evolution from the molds indicated that the molds were completely filled, at which time the filled molds were removed from vacuum and placed in a 120°C oven for

2 hours. Following an overnight cool-down to room temperature, the epoxy replica was released by peeling the PDMS mold from the epoxy.

2.4 Formation of the Control Surface

A pre-cleaned glass slide was placed on a spinner. A 25 mm diameter droplet of the degassed epoxy formulation was placed on the center of the slide. The epoxy was spin-cast until it formed a uniform layer across the glass slide. The coated glass slide was placed in a 120°C oven for 2 hours after which it was allowed to cool to room temperature overnight.

2.5 Contact Angle Measurement Procedure

Contact angle measurements were performed using a contact angle goniometer (originally manufactured by Connelly Applied Research but recently modified by the author). The modifications included the installation of a new video camera (uEye, IDS) and new software (ImageJ [33] and DropSnake [34]). The substrate of interest was placed in the sample chamber and a 1.0-1.4 microliter drop of deionized water was placed on the substrate surface, as per the sessile drop technique. Significant effort was taken to maintain drop volume consistency but some surfaces proved extremely difficult to achieve drop deposition on the surface and a larger drop volume was necessary to overcome capillary adhesion of the water to the syringe tip. Video was taken of the drop deposition as well as of increasing and decreasing the drop size from 0.4 microliter-2.0

microliters. In addition, images were taken of drop evaporation. Static contact angle measurements were taken from images taken immediately after the drop deposition.

2.5.1 Image Analysis

Video was first opened in MATLAB and frames of interest were extracted as pgm files. These images, as well as independently taken stills were then analyzed in ImageJ using the plug-in DropSnake [34]. DropSnake utilizes the entire circumferential drop profile-excluding the region in contact with the surface-to calculate the contact angle. It does this through the use of splines. One uses the software by opening the image of interest in ImageJ. The plug-in DropSnake is then opened. The user first places knots along the drop upper perimeter and then at two locations that appear to be the apex of the contact angle. Among the advantages of using this plug-in is that if one has accurately placed the knots along the drop perimeter, the software effectively places the drop-surface contact points for the user, because placing the drops in egregious positions warps the rest of the curve. The curve is then "snaked" and the calculated contact angles result [34].

2.6 Scanning Electron Microscopy

Following the completion of all contact angle measurements, replicated lotus surfaces were sputter-coated with iridium for 30 seconds and then examined using scanning electron microscopy (Hitachi 4300 SE). The accelerating voltage used was between 2.0-3.0 kV. All images were taken using a tilt angle of 45 degrees.

2.7 Optical Profilometry

Flat epoxy surfaces were examined using an optical profilometer (STIL Micromeasure Optical Profilometer) to determine surface roughness. A 1μL drop has a radius of approximately 1 mm. To that end, a 2 mm x 2 mm area of each surface under investigation was mapped to create a surface roughness profile. Given that the surfaces under investigation appear smooth to the naked eye, the 350μm lens system was used in this investigation. The z-resolution of this lens is 10 nm with an accuracy of 60 nm and a spot diameter of 5.2μm with a lateral resolution of 2.6μm. Each control surface was scanned laterally in 1μm steps across a 2 mm distance, and longitudinally in 5μm or 100μm steps across a 2 mm distance.

Optical profilometry functions by shooting a beam of light at the surface under investigation, and then characterizes the surface by the reflection that bounces back into the lens. Most of the epoxy samples are transparent and do not intrinsically reflect light. To improve the surface reflectivity and improve the measured signal intensity, the samples were sputter-coated with Iridium for 30 seconds prior to undergoing optical profilometry.

CHAPTER 3

RESULTS

Static contact angle measurements, roughness profiles, and scanning electron microscopy images are provided below. Advancing and receding contact angles and a discussion of contact angle hysteresis of water on the fabricated surfaces are beyond the scope of this paper.

3.1 Static Contact Angles

Table 3.1 Summarizes the average measured static contact angle and error for each epoxy formulation for both the flat (i.e. control) and lotus-molded surfaces.

Material	Surface Topography	Average Static Contact Angle	Standard Deviation
Neat epoxy/amine	Control	61.90	5.41
Neat epoxy/amine	Lotus replica	123.11	12.53
5 phr CTBN/epoxy/amine	Control	82.511	2.92
5 phr CTBN/epoxy/amine	Lotus replica	127.24	8.11
10 phr CTBN/epoxy/amine	Control	82.84	6.52
10 phr CTBN/epoxy/amine	Lotus replica	123.02	7.11
20 phr CTBN/epoxy/amine	Control	85.13	3.13
20 phr CTBN/epoxy/amine	Lotus replica	133.27	9.44
0.66 wt% NS/epoxy/amine	Control	70.75	1.45
0.66 wt% NS/epoxy/amine	Lotus replica	109.00	14.16
1.3 wt% NS/epoxy/amine	Control	77.32	1.59
1.3 wt% NS/epoxy/amine	Lotus replica	92.16	13.90
2.56 wt% NS/epoxy/amine	Control	77.64	2.17
2.56 wt% NS/epoxy/amine	Lotus replica	126.46	18.03
4.93 wt% NS/epoxy/amine	Control	80.49	1.29
4.93 wt% NS/epoxy/amine	Lotus replica	136.53	13.10

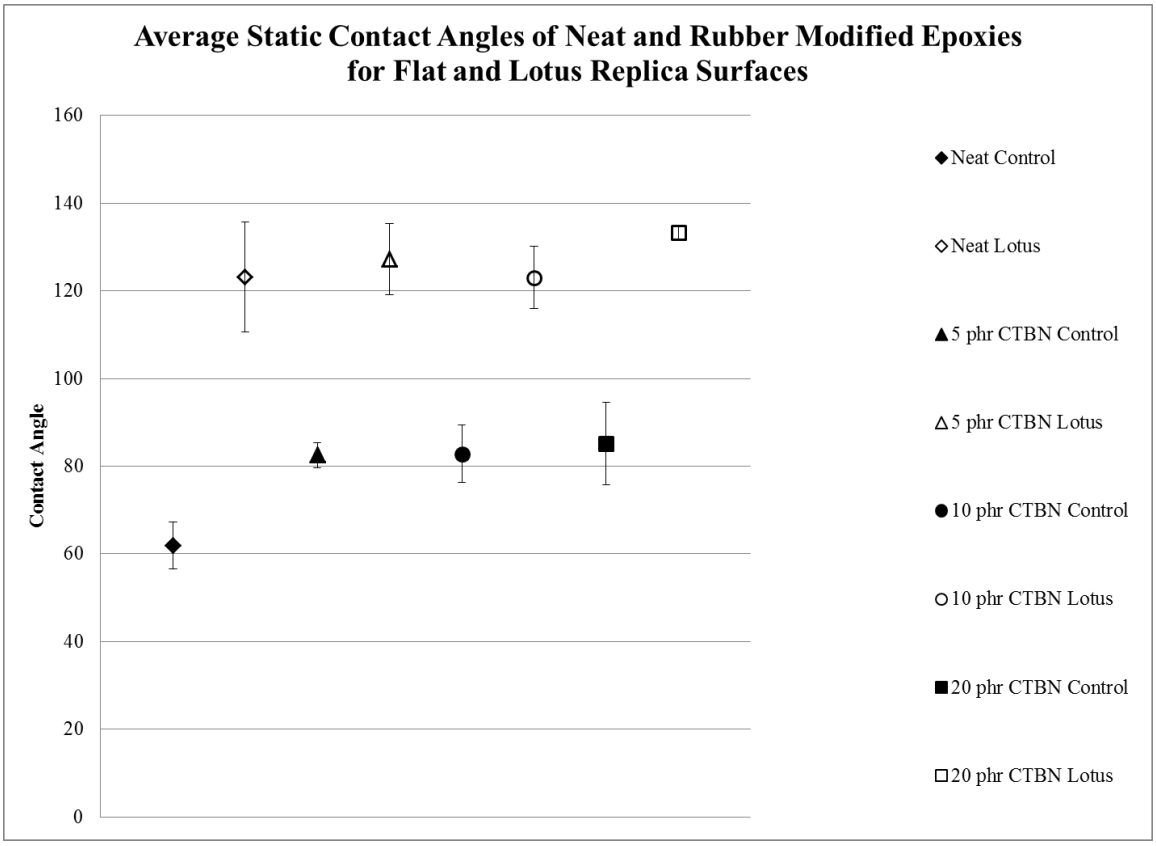

Figure 3.1 Plot of the average static contact angle measurements for the neat and rubber modified epoxies, respectively. The error bars reflect the standard deviation. Please note that for points where the error bars are not readily apparent it means that the standard deviation was small enough to not be discernible on the scale presented.

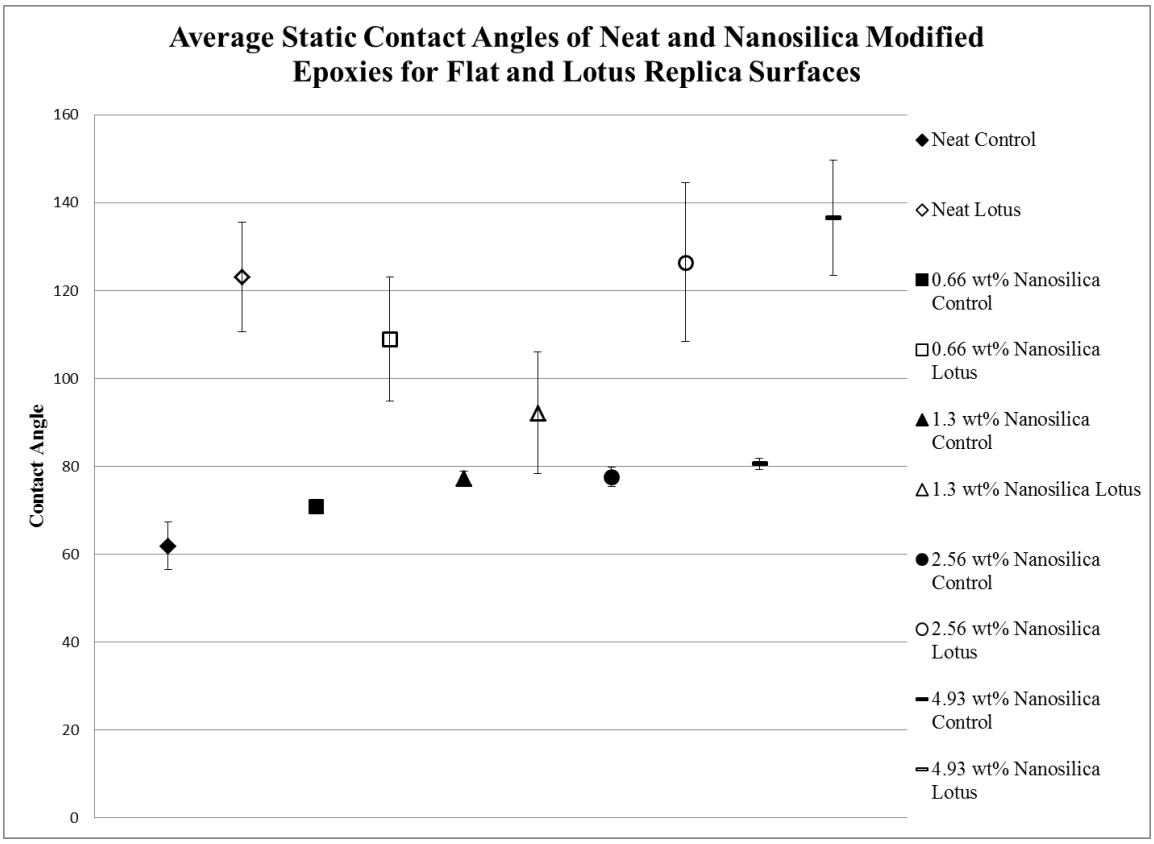

Figure 3.2 Plot of the average static contact angle measurements for the neat and nanosilica modified epoxies, respectively. The error bars reflect the standard deviation. Please note that for points where the error bars are not readily apparent it means that the standard deviation was small enough to not be discernible on the scale presented.

3.2 Scanning Electron Microscopy Images of Lotus-Like Surfaces

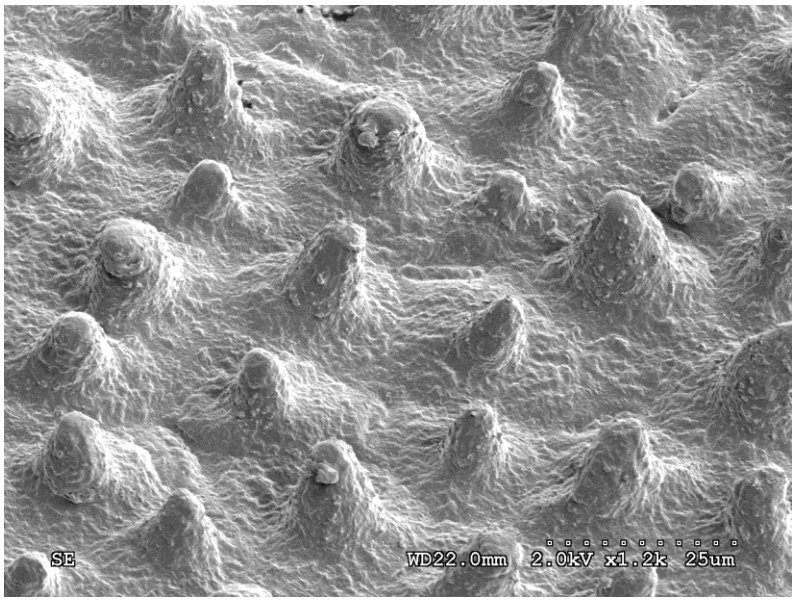

Figure 3.3 Image of a neat epoxy/amine lotus leaf replica surface.

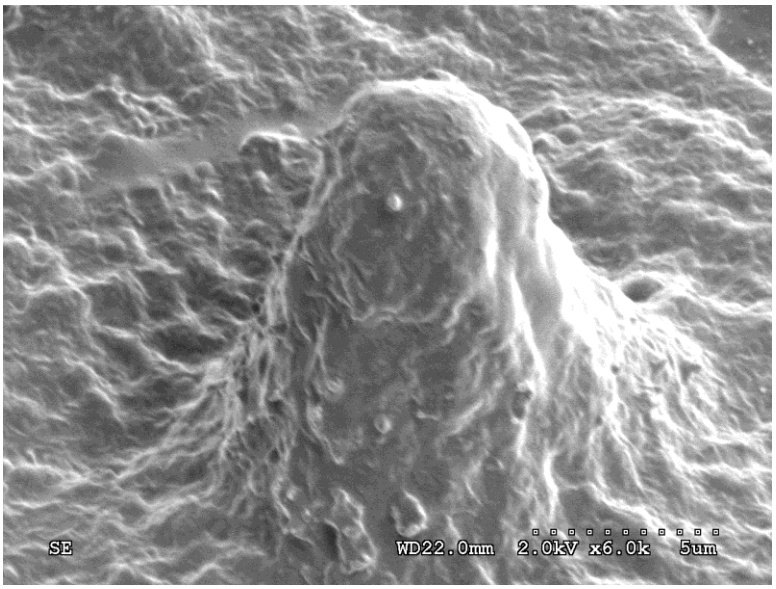

Figure 3.4 Close-up image of a neat epoxy/amine lotus replica papilla.

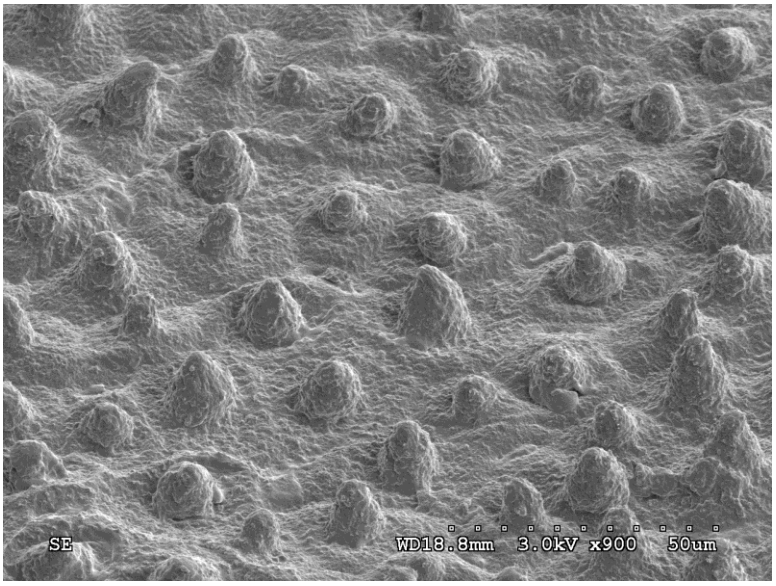

Figure 3.5 Image of a 5 phr CTBN/epoxy/amine lotus leaf replica surface.

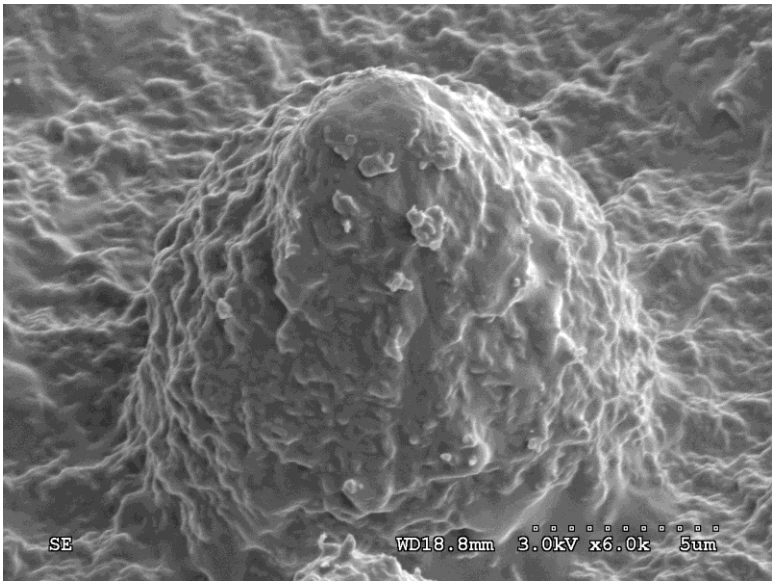

Figure 3.6 Close-up image of a 5 phr CTBN/epoxy/amine lotus replica papilla.

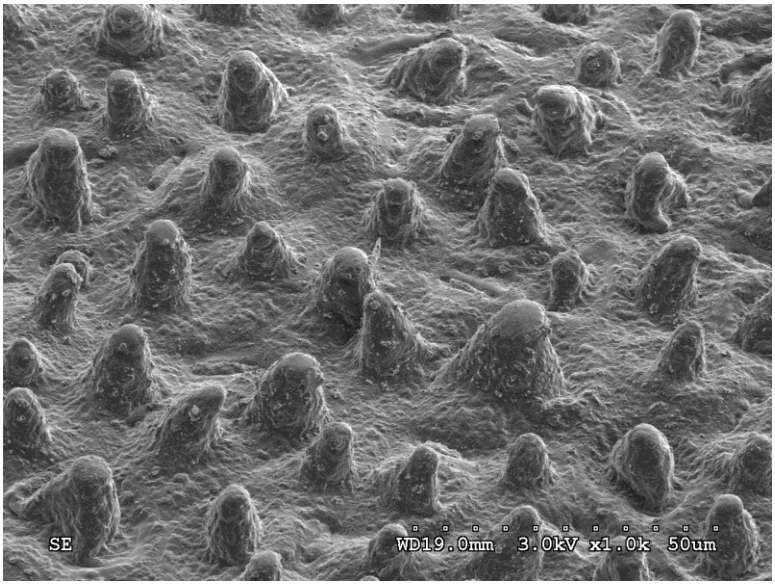

Figure 3.7 Image of a 10 phr CTBN/epoxy/amine lotus leaf replica surface.

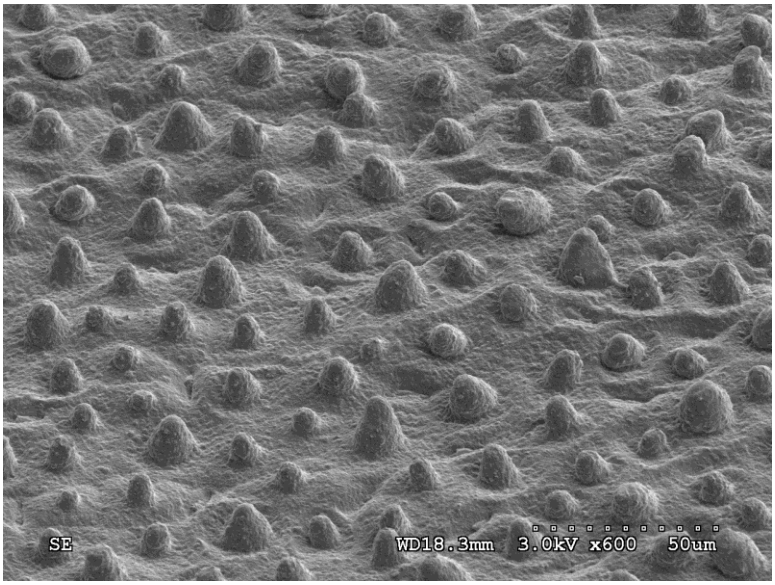

Figure 3.8 Image of a 10 phr CTBN/epoxy/amine lotus leaf replica surface.

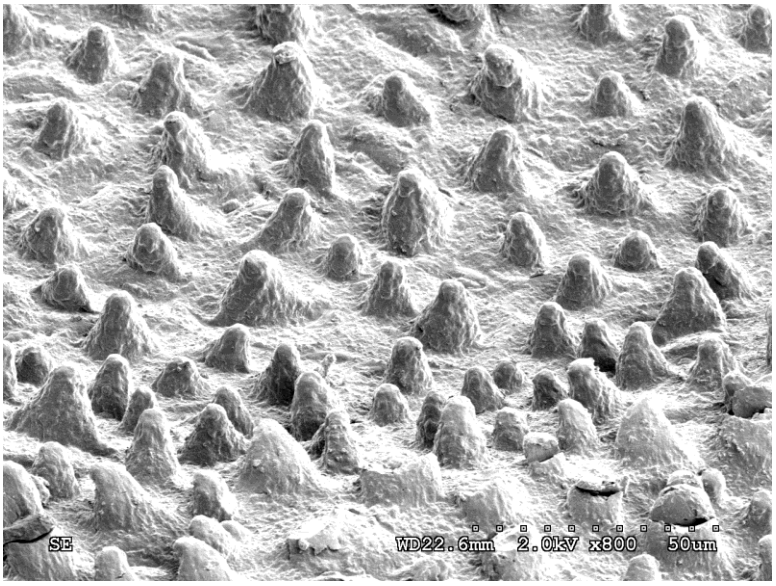

Figure 3.9 Image of a 0.66 wt% Nanosilica/epoxy/amine lotus leaf replica surface.

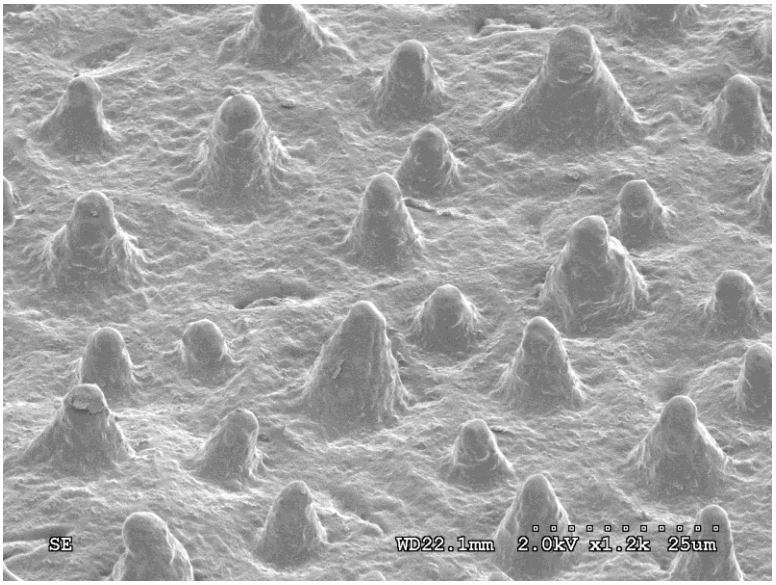

Figure 3.10 Image of a 1.3 wt% Nanosilica/epoxy/amine lotus leaf replica surface.

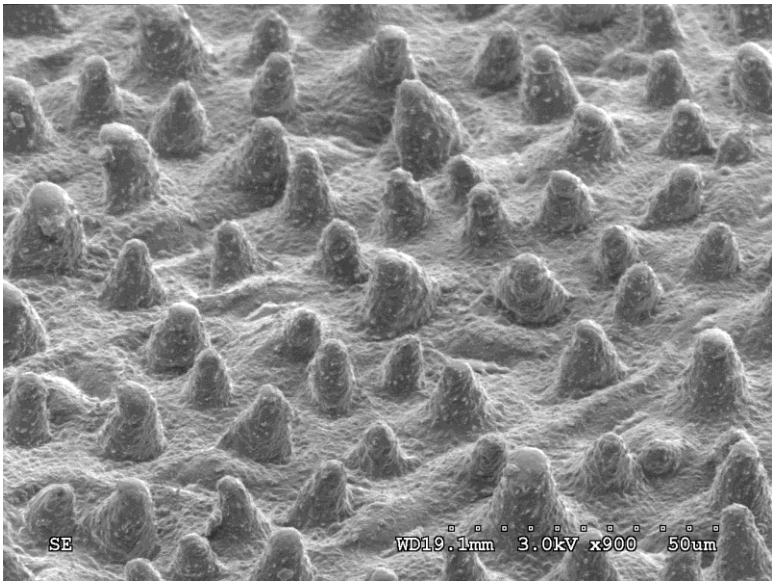

Figure 3.11 Image of a 2.56 wt% Nanosilica/epoxy/amine lotus leaf replica surface.

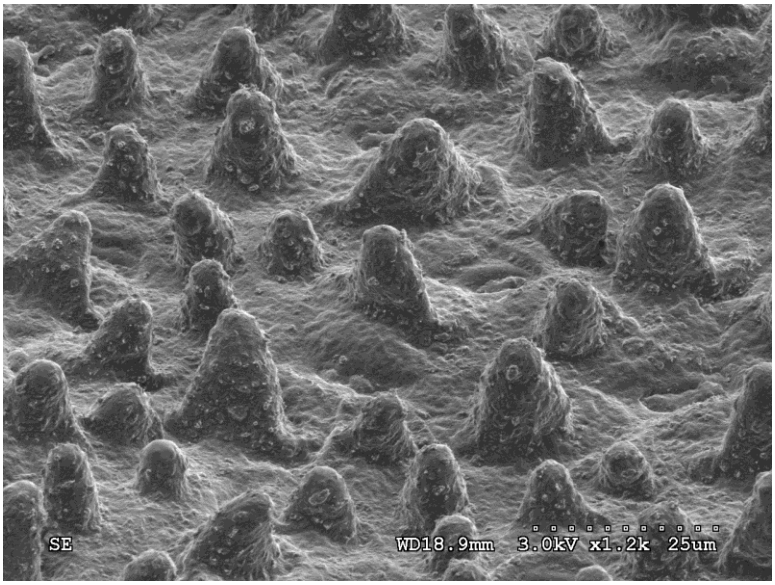

Figure 3.12 Image of a 4.93 wt% Nanosilica/epoxy/amine lotus leaf replica surface.

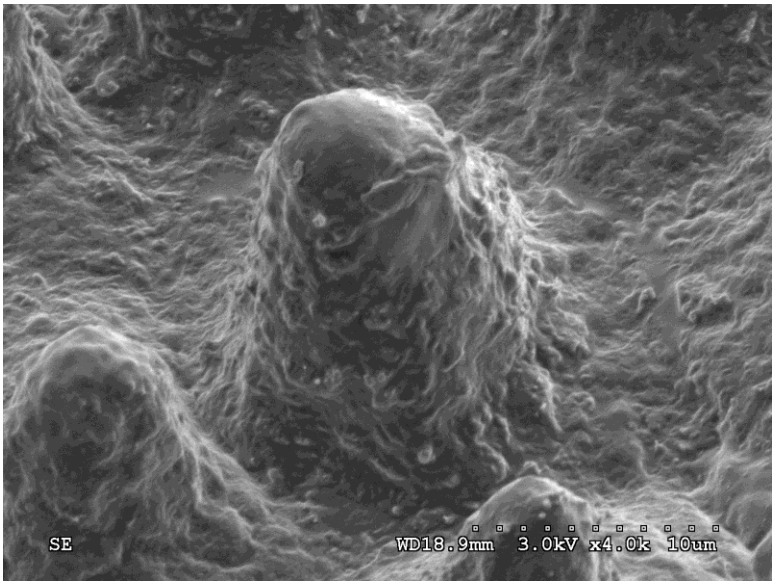

Figure 3.13 Close-up image of a 4.93 wt% Nanosilica/epoxy/amine lotus replica papilla.

3.3 Profiles of Control Surfaces

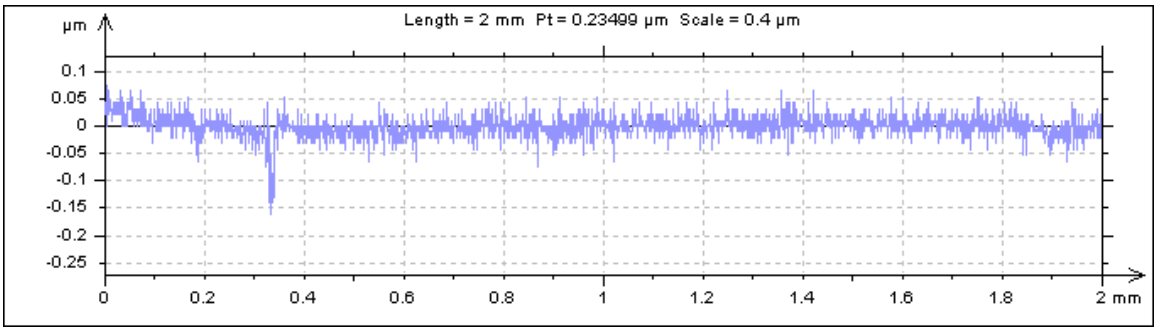

Figure 3.14 Optical profilometry results for a flat neat amine-cured epoxy system. The examined area is 2 mm x 2 mm. The step in the x-direction is 1 µm and the step in the y-direction is 100 µm. The profile plot is the average of 20 scans.

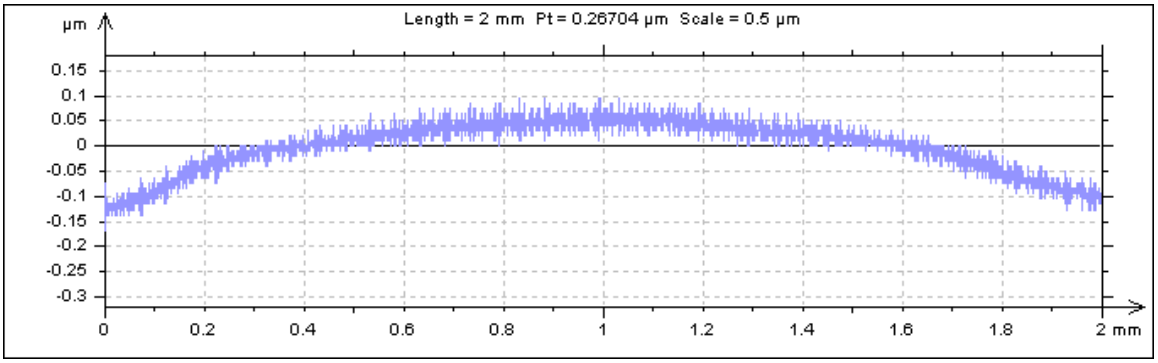

Figure 3.15 Optical profilometry results for a flat 0.66 wt% nanosilica-modified amine-cured epoxy system. The examined area is 2 mm x 2 mm. The step in the x-direction is 1 µm and the step in the y-direction is 5 µm. The profile plot is the average of 400 scans.

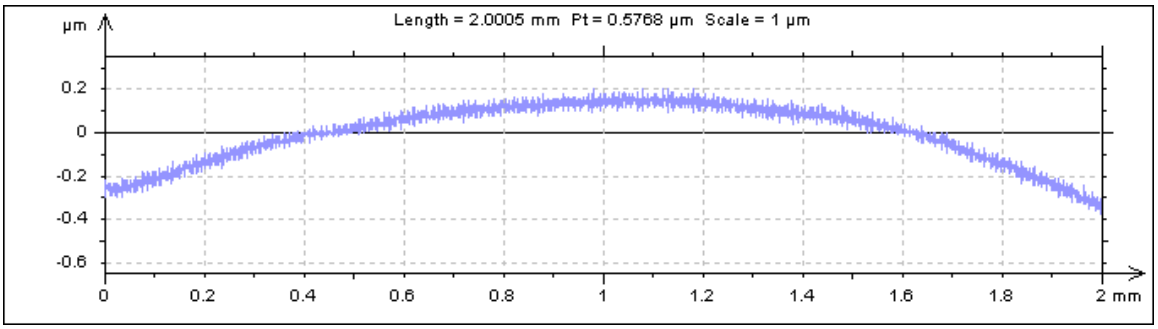

Figure 3.16 Optical profilometry results for a flat 1.3 wt% nanosilica-modified amine-cured epoxy system. The examined area is 2 mm x 2 mm. The step in the x-direction is 1 µm and the step in the y-direction is 5 µm. The profile plot is the average of 400 scans.

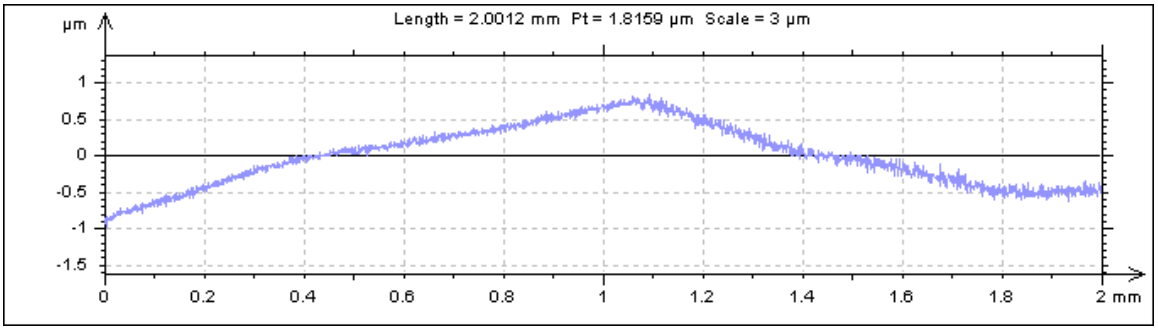

Figure 3.17 Optical profilometry results for a flat 4.93 wt% nanosilica-modified amine-cured epoxy system. The examined area is 2 mm x 2 mm. The step in the x-direction is 1 µm and the step in the y-direction is 100 µm. The profile plot is the average of 20 scans.

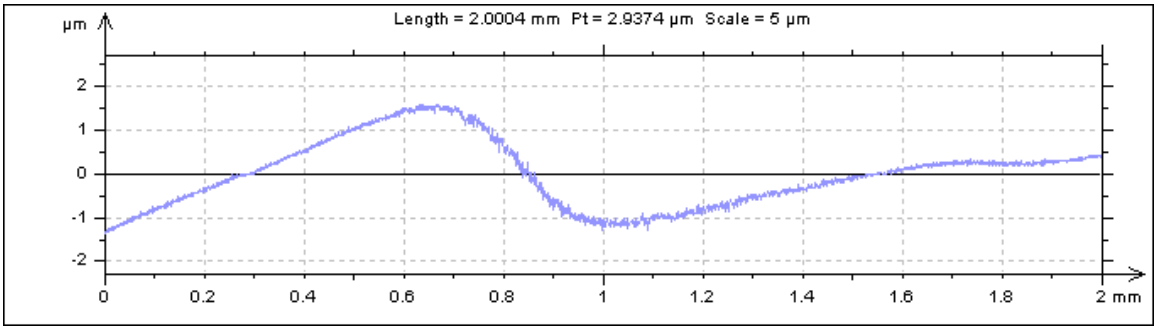

Figure 3.18 Optical profilometry results for a flat 5 phr CTBN-modified amine-cured epoxy system. The examined area is 2 mm x 2 mm. The step in the x-direction is 1 µm and the step in the y-direction is 100 µm. The profile plot is the average of 20 scans.

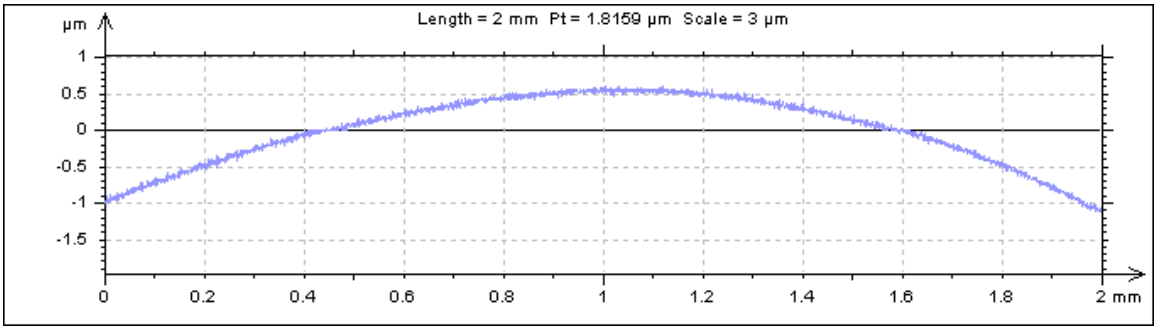

Figure 3.19 Optical profilometry results for a flat 10 phr CTBN-modified amine-cured epoxy system. The examined area is 2 mm x 2 mm. The step in the x-direction is 1 µm and the step in the y-direction is 100 µm. The profile plot is the average of 20 scans.

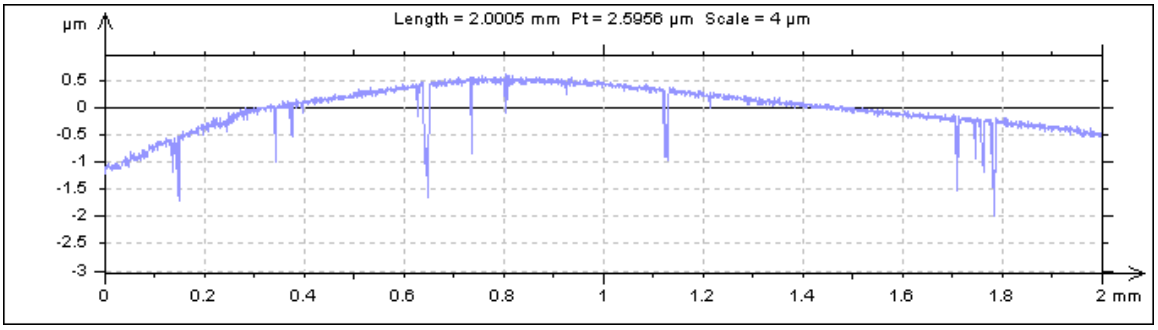

Figure 3.20 Optical profilometry results for a flat 20 phr CTBN-modified amine-cured epoxy system. The examined area is 2 mm x 2 mm. The step in the x-direction is 1 µm and the step in the y-direction is 100 µm. The profile plot is the average of 20 scans.

CHAPTER 4

DISCUSSION

This section elaborates on the results of the replica molding, static contact angle measurements, and optical profilometry that were provided in Chapter 3.

4.1 Replica molding

From the results of this experiment, it is clear that it is possible to form a lotus-like surface from epoxy using the replica molding technique. The scanning electron microscopy images reveal that the replicas have the same micron-scale morphology as the original leaf. At the same time, the wax tubules that render the leaf of the *Nelumbo nucifera* superhydrophobic were not replicated with any degree of fidelity to the original. It is most likely the lack of this compound morphology that prevented the epoxy lotus replicas from having a superhydrophobic surface [35].

It is theorized that the rough patterned surface on the sides of the papillae and on the replicated base epidermal cells are derived from the wax tubules; they may have been crushed during the molding process-but this is unknown conclusively at this time. The smooth papillae tips imply that the morphology of the wax tubules was not successfully duplicated in that area by the epoxy. It is theorized that the nonacosonal wax tubules were removed from the tips of the papillae while peeling the PDMS mold from the original lotus leaf. With the wax tubules embedded in the PDMS mold, there would not

be any opportunity for the epoxy to fill a void. Similar difficulties of crushed or lost nonacosanol tubules during replica molding were reported by Koch et al [10].

Figures 3.3-3.13 show that regardless of epoxy formulation, the replicated lotus surfaces appear essentially the same, even unto the roughness of the individual papillae and on the base epidermal cells. This surface uniformity despite material chemistry changes is reflected in the static contact angle results, with essentially the same static contact angle being found for each replicated lotus surface.

The only exception to uniformity of measured static contact angles is the 1.3 wt% nanosilica/epoxy/amine formulation of the replicated lotus leaf. The average static contact angle for this sample was lower than the other replicated lotus surfaces. Inspecting the surface following the conclusion of experimentation, it was found that a replicated leaf vein was running through the middle of the sample surface. The leaf vein has larger dimensions than do the papillae and could have provided sites for encouraging wetting, thus resulting in lower measured contact angles.

4.2 Optical Profilometry

Much difficulty was encountered in the execution of the optical profilometry measurements. The small feature size on the control surfaces necessitated using the 350 μm lens system but even with sputtering the samples with iridium prior to testing, the signal intensity was barely above a threshold value (i.e. 3-4% intensity instead of 30+%).

Additional difficulties were created by the software that controls the system, wherein a test executed multiple times with identical settings would take a varying amount of time to complete, with the variance on the order of hours.

A 2 mm x 2 mm map was made of each control surface with the intent of determining surface uniformity and surface roughness within the area that a 1 µL drop would encompass. However, because of the difficulties described above the number of scans across the 2 mm x 2 mm area are not consistent among all of the control surfaces. The data presented in Figures 3.14-3.20 are profiles of the 2 mm x 2 mm area, averaged across the y-direction. The plots show that the peak-valley distance for every control surface across a 2 mm line in the x-direction does not exceed 3 µm, and the peak-valley distance is typically much less than that. These distances are much less than those of the lotus replicas, where papillae are usually not less than 10 µm tall.

The optical profilometry results support the static contact angle measurements: namely, the spin-cast control surface is more uniform in terms of peak-valley distance than the epoxy lotus replica surfaces, and these conditions encourage wetting in the Wenzel regime. Homogeneous wetting gives rise to drop spreading on the surface, and lower contact angles.

CHAPTER 5

SUMMARY

It was found that it is possible to use the replica molding technique to create a lotus-like surface using neat, CTBN-modified and nanosilica-modified epoxies. These epoxy lotus-like surfaces were characterized using the sessile drop technique to measure the static contact angle of water on the surface, and it was found that the lotus replicas had an increase in static contact angle of approximately 40 degrees over their spin-cast counterparts. In addition, it was found that surface topography dominated the effects of surface chemistry, with the replicated lotus surfaces having essentially the same static contact angle, irrespective of the epoxy formulation.

This work demonstrated that it is possible to take a typically hydrophilic surface like epoxy and by modifying the surface morphology attenuate the affinity of water to wet its surface. Further work will include defining the contact angle hysteresis of the surface through measuring the advancing and receding contact angles of water on the surface.

CHAPTER 6

REFERENCES

1. B. Mockenhaupt, H.-J. Ensikat, M. Spaeth, W. Barthlott, *Langmuir*, **24** (2008) 13591.
2. W. Barthlott and C. Neinhuis, *Planta*, **202** (1997) 1.
3. P. Wagner, R. Fürstner, W. Barthlott, C. Neinhuis, *J Exp Bot* **54** (2003) 1295.
4. K. Koch, B. Bhushan, W. Barthlott, *Soft Matter* **4** (2008) 1943.
5. C. Neinhuis, W. Barthlott, *Ann Bot* **79** (1997) 667.
6. K. Koch, H. F. Bohn, W. Barthlott, *Langmuir* **25** (2009) 14116.
7. H. Bargel, K. Koch, Z. Cerman, C. Neinhuis, *Funct Plant Biol* **33** (2006) 893.
8. H. J. Ensikat, M. Boese, W. Mader, W. Barthlott, K. Koch, *Chem Phys Lipids* **144** (2006) 45.
9. H. J. Ensikat, P. Ditsche-Kuru, C. Neinhuis, W. Barthlott, *Beilstein J Nanotechnology* **2** (2011) 152.
10. K. Koch, B. Bhushan, Y.C. Jung and W. Barthlott, *Soft Matter*, 5 (2009) 1386.
11. M. Adithyavairavan and S. Subbiah, *Surf Coat Tech*, 205 (2011) 4764.
12. S.-M. Lee and T.H. Kwon, *J Micromech Microeng*, 17 (2007) 687.
13. G. Jin and G.H. Kim, *Langmuir*, 27 (2011) 828.
14. V. Zorba, E. Stratakis, M. Barberoglou, E. Spanakis, P. Tzanetakis, S. H. Anastasiadis, C. Fotakis, *Adv Mater*, 20 (2008) 4049.
15. B. Bhushan, Y. C. Jung, and M. Nosonovsky, Springer Handbook of Nanotechnology 3rd Edition (2010) 1437.

16. A.J. Kinloch *Adhesion and Adhesives Science and Technology*, Chapman and Hall, London, 1987.
17. R. N. Wenzel, *Ind Eng Chem,* 28 (1936) 988.
18. A. B. D. Cassie, S. Baxter, *Trans Faraday Soc* **40** (1944) 546.
19. B. Bhushan, Y. J. Chae, *Ultramicroscopy* **107** (2007) 1033.
20. Y. Zhang, Y. Chen, L. Shi, J. Li, Z. Guo, *J Mater Chem* **22** (2012) 799.
21. D. Ebert, B. Bhushan, *J Colloid Interface Sci* **368** (2012) 584.
22. M. Ma, R. M. Hill, *Curr Opin Colloid In* **11** (2006) 193.
23. B. Bhushan, Y. C. Jung, K. Koch, *Phil Trans R Soc A* **367** (2009) 1631.
24. B. Bhushan, Y. C. Jung, *Prog Mater Sci* **56** (2011) 1.
25. X.-M. Li, D. Reinhoudt, M. Crego-Calama, *Chem Soc Rev* **36** (2007) 1350.
26. Y. Xia, J. J. McClelland, R. Gupta, D. Qin, X.-M. Zhao, L. L. Sohn, R. J. Celotta, G. M. Whitesides, *Adv Mater* **9** (1997) 147.
27. M. Sun, C. Luo, L. Xu, H. Ji, Q. Ouyang, D. Yu, Y. Chen, *Langmuir* **21** (2005) 8978.
28. R. A. Singh, H. J. Kim, J. Kim, S. Yang, H. E. Jeong, K. Y. Suh, E.-S. Yoon, *J Mech Sci Technol* **21** (2007) 624.
29. R. A. Singh, E.-S. Yoon, H. J. Kim, J. Kim, H. E. Jeong, K. Y. Suh. *Mat Sci Eng C* **27** (2007) 875.
30. G. Jin, H.J. Jeon, G. H. Kim, *Soft Matter* **7** (2011) 4723.
31. Z. Yuan, H. Chen, J. Zhang, *Appl Surf Sci* **254** (2008) 1593.
32. R. Fürstner, W. Barthlott, C. Neinhuis, P. Walzel, *Langmuir* **21** (2005) 956.
33. Rasband, W.S., ImageJ, U. S. National Institutes of Health, Bethesda, Maryland,

USA, http://imagej.nih.gov/ij/, 1997-2012

34. A. F. Stalder, G. Kulik, D. Sage, L. Barbieri, P. Hoffmann, *Colloid Surface A* **286** (2006) 92.

35. M. Nosonovsky, B. Bhushan, *Microelectron Eng* **84** (2007) 382.

CHAPTER 7

VITA

Maria Martine Salamon was born in Pennsylvania, in May 1982 to John and Mary Salamon. She graduated from Emmaus High School in 2000.

In 2004, Maria received her Bachelor of Science and Engineering degree with a major in Materials Science and Engineering and Minors in Macromolecular Science and Engineering and Psychology, respectively, from Case Western Reserve University in Cleveland, Ohio.

In 2006, she matriculated at Lehigh University as a part-time Distance Education student. In the course of her studies she formally joined the Polymer Science and Engineering Graduate Program under the guidance of Dr. Raymond A. Pearson.